Comparative analysis of SCIG and DFIG Based Wind Generation on Transient Stability of the Kenyan Power System

Orenge R. S., Muriithi C. M., Nyakoe G. N. and Muisyo I. N.

Abstract—Generation of Electrical power from wind is achieved using the two mainly available generator technologies. These technologies are the squirrel cage induction generators (SCIG) and doubly fed induction generators (DFIGs). In this paper, the effect of wind farms employing these two technologies on the transient stability of a power systems was investigated. Simulations were carried out to demonstrate and compare the transient performance of Kenyan power system with the two wind generator technologies during a three phase fault. The two generator technologies mentioned were analyzed separately to establish which one of then will least impact the Kenyan Power system. The location and the capacity of the wind farm was informed by the proposed Lake Turkana Wind Power project which is expected to add 300 MW of power to the Kenyan grid. The system was established and all the analysis carried out in the power system analysis tool DIgSILENT PowerFactory. The results show that a better transient performance will be achieved in the case of a DFIG based wind farm, compared to the one based on SCIG.

Keywords—Syncronous generators, Doubly-fed induction generators (DFIG), Transient stability, settling time, wind farm.

I. INTRODUCTION

RENEWABLE energy technologies are becoming a point of focus in the world today due to depletion of fossil fuels and environmental concerns, among other reasons. Wind power generation as a renewable resource is one of the fastest growing electricity generating technologies and features in energy plans across the world, both in the developed and the developing world. According to the World Wind Energy Association over, 282 GW of capacity is now installed worldwide with China for instance having over 75 GW installed capacity [1], [2]. Some countries have high penetration levels like Denmark which meets about 29% of its power demand from wind [1]. It is also evident that the installed wind energy capacity has been increasing significantly around the world in the recent past. Wind power's rapid expansion has been driven by a combination of its environmental benefits, various state and federal policies and incentives, and improving cost-competitiveness with other traditional generation technologies [3], [4]. Kenya currently has an energy capacity deficit whereby at peak demand there is insufficient generation to meet consumer demand. In addition, demand is growing at 8% per year [5]. The country is suffering from chronic power shortages abated only by expensive diesel generated power. The vast majority of Kenya's electric power capacity is based on hydropower, the rest of the country's power requirements is supplied by geothermal and thermal power plants. The over reliance on hydropower means that supply is often unreliable, especially during the dry seasons [5]. The Kenyan government through the Energy Act of 2006 emphasizes on the need to encourage development of renewable energy resources of which wind is one of these technologies. Through this act, the Ministry of Energy is mandated with the task of promoting the development of appropriate local capacity for the manufacture, installation, maintenance and operation of basic renewable technologies such as wind [6]. Integration of large quantities of wind power can however present some challenges and this may affect system stability especially in weak power grids.

Orenge R. S., Department of Electrical and Electronic Engineering, DKUT (Phone: +254722802207; e-mail: samroyoin@gmail.com).
Muriithi C. M., Department of Electrical and Electronic Engineering, JKUAT (e-mail: cmmuriithi@eng.jkuat.ac.ke).
Nyakoe G. N., Department of Mechatronic Engineering, JKUAT (e-mail: nyakoe@eng.jkuat.ac.ke).
Muisyo I. N., Department of Electrical and Electronic Engineering, JKUAT (e-mail: muisyoirene@jkuat.ac.ke).

II. GENERATION TECHNOLOGIES

Induction generators are the most commonly used generators in wind turbines because they are cheap and widely available [7]. Two kinds of induction generators are normally used in wind turbines, namely:

1) Squirrel cage induction generators (SCIGs).
2) Doubly fed induction generator (DFIGs).

The operational characteristics of these two kinds of technologies is described in the following paragraphs.

A. Squirrel Cage Induction Generators

Wind turbines based on this technology are directly coupled to the grid as shown in Figure 1 below.

The slip, and hence the rotor speed of a squirrel cage induction generator varies with the amount of power generated. These rotor speed variations are, however, very small, approximately 1 to 2 per cent. Therefore, this type of wind turbine is normally referred to as a constant speed or fixed speed turbine. A squirrel cage induction generator always consumes reactive power. In most cases, this is undesirable, particularly in the case of large turbines and weak grids. Reactive power consumption of the squirrel cage induction generator is nearly always partly or fully compensated by capacitors in order to achieve a power factor close to one [8].

The equivalent circuit of the SCIG used in DIgSILENT is shown in Figure 2

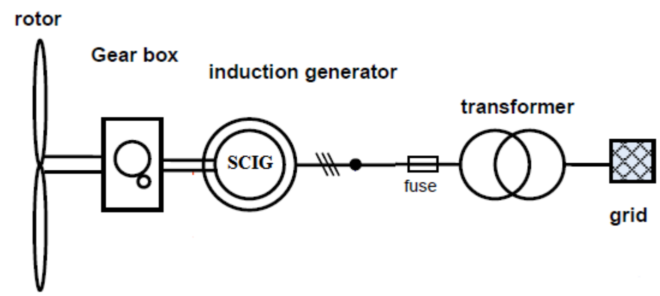

Fig. 1. *Grid connected Squirrel cage induction generator.*

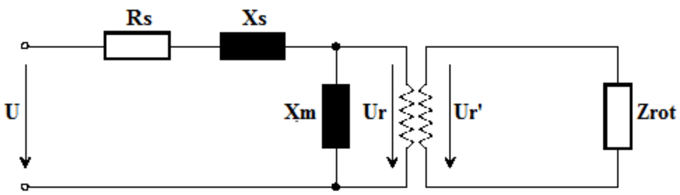

Fig. 2. *Equivalent circuit of a squirrel cage induction generator.*

The model is characterized by the stator winding resistance Rs, the stator leakage reactance X_s, the magnetizing reactance X_m, the rotor impedance Z_{rot}, the stator terminal voltage U, and ring voltage of the rotor U_r.

The dynamic model of the induction generator uses the steady state parameters defined in the equivalent diagram depicted in Figure 2. DIgSILENT provides a $d-q$ model, expressed in the rotor reference frame:

$$u_s = R_s i_s + j\omega_{syn}\psi_s + \frac{d\psi_s}{dt}$$
$$0 = R_r i_r + j(\omega_{syn} - \omega_r)\psi_r + \frac{d\psi_r}{dt} \quad (1)$$

where u, i, and ψ are space vectors for the voltage, current and flux, respectively. ω_{syn} is the synchronous speed, while ω_r is the angular speed of the rotor. As the rotor is short-circuited in the squirrel-cage induction generator, the rotor voltage is set to zero. The generator inertia is specified in the form of an acceleration time constant in the induction generator type. The dynamic model of the induction generator is completed by the mechanical equation [9]:

$$J\dot{\omega}_r = T_e - T_m \quad (2)$$

where J is generator inertia, T_e is the electrical torque, T_m is the mechanical torque. The mechanical equation can be rated to the nominal torque:

$$T_n = \frac{P_n}{[\omega_n(1 - s_n)]} \quad (3)$$

and thus the acceleration time constant T_{ag} can be expressed as:

$$T_{ag} = \frac{J(1 - s_n)\omega_n^2}{P_n} \quad (4)$$

where ω_n is the nominal electrical frequency of the network, P_n is the nominal power and s_n is the nominal slip.

B. Doubly-fed induction generator (DFIG)

The DFIG is a wound rotor type of an induction machine whose three phase rotor terminals are connected to back-to-back PWM power converters. The power converters are then connected to the grid. The stator terminals are connected directly to the grid. This is illustrated in Figure 3.

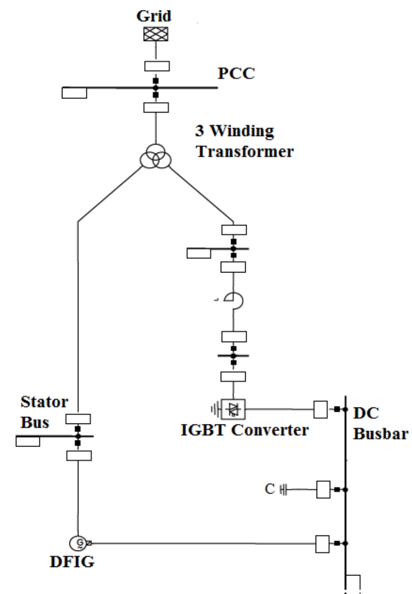

Fig. 3. *Grid connection of doubly fed induction generator.*

In contrast to a conventional, squirrel cage induction generator, the electrical power of a doubly-fed induction machine is independent from the speed. Therefore, it is possible to realize a variable speed wind generator allowing for adjustment of the mechanical speed to the wind speed and hence operating the turbine at the aerodynamically optimal point for a certain wind speed range [10]. The DFIG equivalent circuit is similar to that of a conventional generator except that the rotor circuit includes the power converters. The doubly-fed induction generator (DFIG) model in DIgSILENT equivalent circuit is as illustrated in the Figure 4

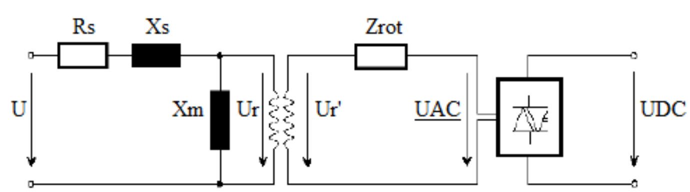

Fig. 4. *Equivalent circuit model of DFIG*

Where:
U is the stator terminal voltage.
Ur The slip ring voltage of the rotor.
UAC The ac rotor slip ring voltage.
UDC The dc voltage on the DC bus of the converter.
Rs Is the stator resistance.
Xs The stator reactance.
Zrot The impedance of the rotor circuit.

The doubly-fed induction generator (DFIG) model shown in figure 4 extends the usual squirrel cage induction generator by a PWM rotor side converter in series with the rotor impedance Zrot. The PWM converter inserted in the rotor circuit allows for a flexible and fast control of the machine by modifying the magnitude and phase angle of the generator's AC voltage output UAC on the rotor side. This is done by modifying the modulation factor PWM. Based on the power balance between the AC and DC side of the converter, the DC voltage and DC current can then be calculated. The AC-DC relationship of the PWM converter is as follows (the AC voltage is expressed as line-to-line voltage):

$$U_{ACr} = \frac{\sqrt{3}}{2\sqrt{2}}.PWM_r.U_{DC}$$
$$U_{ACi} = \frac{\sqrt{3}}{2\sqrt{2}}.PWM_i.U_{DC} \quad (5)$$

where PWM_r and PWM_i are the real and imaginary components of the modulation factor, respectively. U_{ACr} and U_{ACi} are the real and imaginary components of the AC voltage. It is assumed that a standard bridge consisting of six transistors builds the converter and that an ideal sinusoidal pulse width modulation is applied. The relationship between AC and DC currents can be found by assuming that the PWM converter is loss free:

$$P_{AC} = Re(U_{AC}I^*_{AC}) = U_{DC}I_{DC} = P_{DC} \quad (6)$$

During time domain simulations, the converter is controlled through the pulse width modulation factors PWM_d and PWM_q, which define the ratio between DC-voltage and the AC-voltage at the slip rings. The model equations of the doubly fed machine can be derived from the normal squirrel cage induction machine equations by modifying the rotor-voltage equations:

$$\underline{u}_s = \underline{R}_s\underline{i}_s + j\frac{\omega_{syn}}{\omega_n}\underline{\psi}_s + \frac{1}{\omega_n}\frac{d\underline{\psi}_s}{dt}$$
$$u_r e^{-j(\omega_{syn}-\omega_r)t} = \underline{R}_r\underline{i}_r + j\frac{(\omega_{syn}-\omega_r)}{\omega_n}\underline{\psi}_r + \frac{1}{\omega_n}\frac{d\underline{\psi}_r}{dt} \quad (7)$$

The per unit rotor voltage that appears in the above equation is related to the DC- voltage as follows:

$$\underline{u}_{rd} = \frac{\sqrt{3}}{2\sqrt{2}}.PWM_d.\frac{U_{DC}}{U_{rnom}} \quad (8)$$
$$\underline{u}_{rq} = \frac{\sqrt{3}}{2\sqrt{2}}.PWM_q.\frac{U_{DC}}{U_{rnom}}$$

where U_{rnom} is the nominal rotor voltage.

III. CASE STUDY

A. Test Power System Model

The original Kenyan system was drawn in DIgSILENT power factory, as shown in figure 5. This network is drawn with 44 buses in accordance to the most currently available data. In this network, only the 220 kV buses and 132 kV buses were represented. The few 11 kV buses are generation buses (PV buses). The Kenyan Power system has an Installed capacity of about 1500 MW. The proposed Lake Turkana Wind Project (LTWP) which aims at providing 300 MW of wind power to the system was also modelled and included in the system. The wind farm was modelled with both the SCIG and DFIG at a time. To investigate and compare the impact of the two wind farms separately, we looked at the transient response of the system to a fault with each technology being monitored separately. An assumption was made that wind speed is constant and the wind turbines were producing their maximum rated power. It is also assumed that all the 300 MW is injected at once. A three phase short circuit was applied on the Dandora to Nairobi North 220 KV transmission line at 50% distance. The fault was cleared by tripping the line at both ends. This was repeated in both cases (i.e. with each technology). Analysis on each of the above cases was carried out separately. The post fault behaviour of different generators in the system was observed considering different parameters such as the active power, reactive power, terminal voltage and the rotor angle of these generators. The action of the excitation control was not considered in this study.

B. Transient Stability Indices

One way of telling the severity of a system fault is looking at how long it takes for the system to regain its initial state of operation. This is indicated by the settling time. This can only be realized if a fault is cleared before reaching the critical clearing time. A system which takes less time to settle is said to be more stable and vice versa. This is the indicator that was used in this study.

IV. Simulations, Results and Discussions

Simulations were carried out to compare the transient response of the active power, reactive power, rotor angle and voltage magnitude with the LTWP wind farm for the two technologies i.e DFIG and SCIG. For the purposes of this paper the active power, reactive power, rotor angle and voltage magnitude after a fault of the Gitaru and Turkwell generation stations were considered.

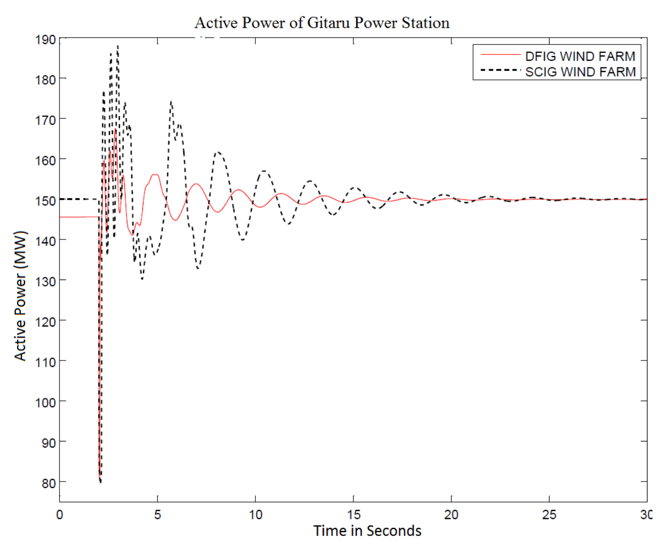

Fig. 6. *Active power of Gitaru Station for both wind farms.*

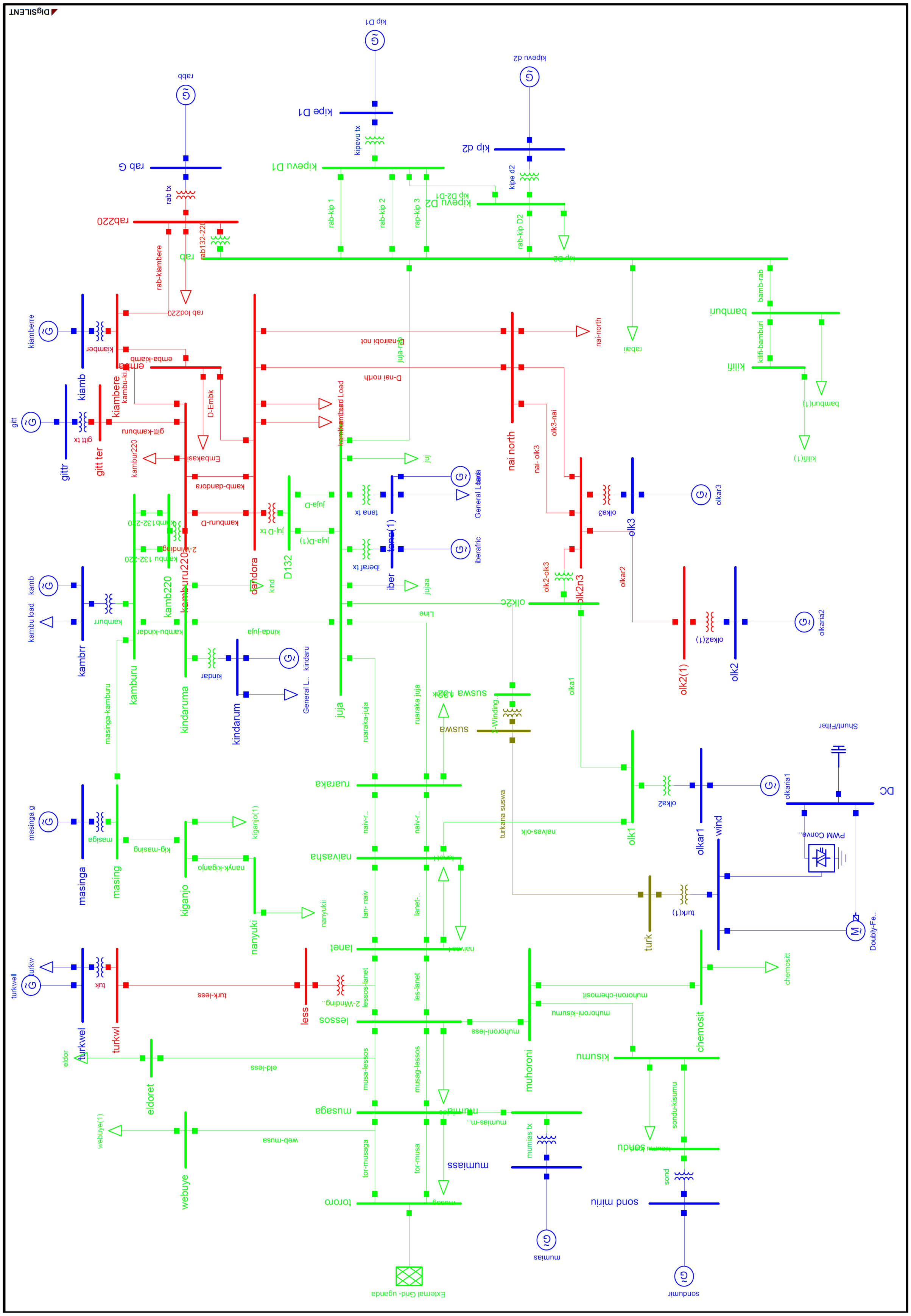

Fig. 5. *Kenyan Power System Transmission Network*

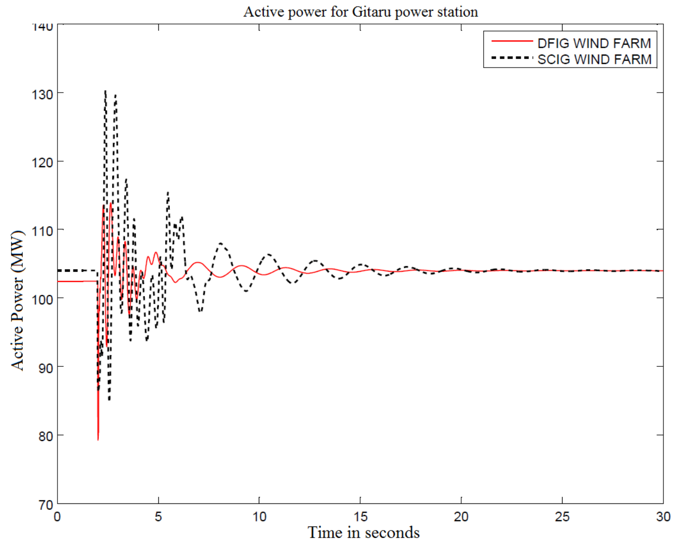

Fig. 7. *Active power of Turkwell Station for both wind farms.*

Figures 6 and 7 compares the active power response of Gitaru and Turkwell power stations respectively. It takes about 16 seconds and 14 seconds for the active power to settle in Gitaru and Turkwel respectively in the case of DFIG wind farm by the end of 30 seconds the system will not have fully settled from the effect of the fault.

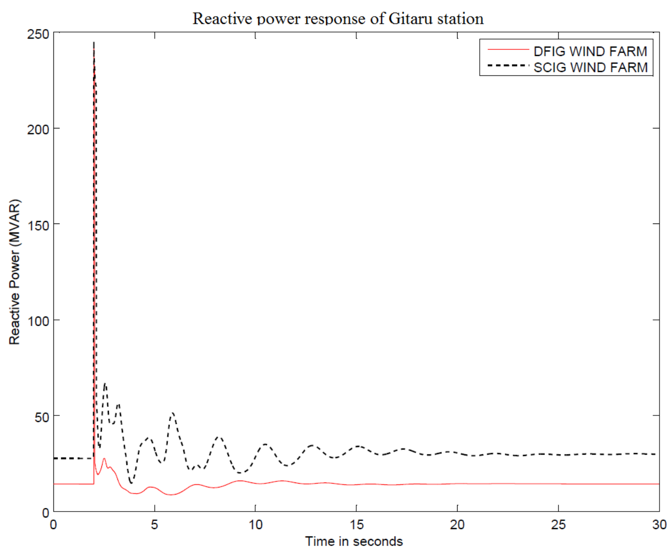

Fig. 8. *Reactive power of Gitaru station for both wind farms.*

Figures 8 and 9 are looking at the reactive power of the two power stations whereby it can be seen than in the case of DFIG wind power integration Gitaru power station will have settled at about 12 seconds while it takes up to about 23 seconds for the same station to regain its normal operation when the system has SCIG based wind farm. On the same figure i.e Figure 9, it was observed that by the 16^{th} second the reactive power in Turkwel had settled considering DFIG wind farm whereas in the case of SCIG the full settling occurs at about the 22^{nd} second.

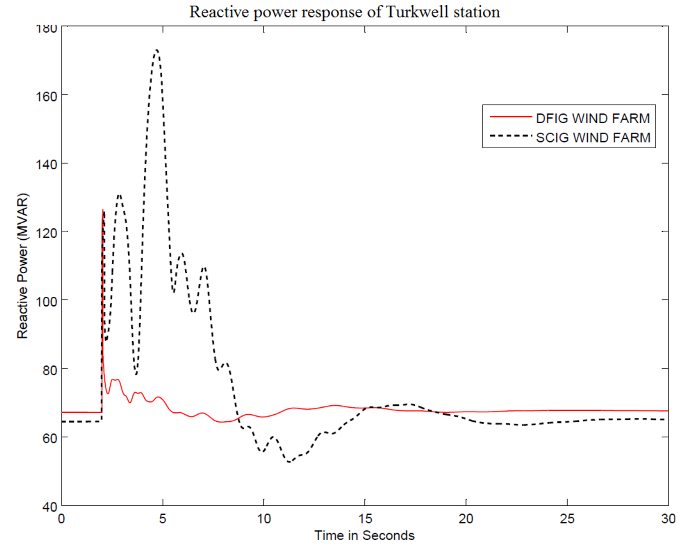

Fig. 9. *Reactive power of Turkwell station for both wind farms.*

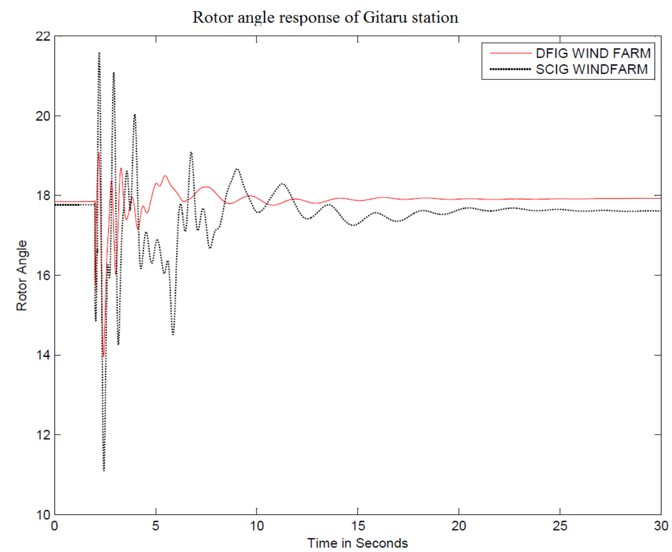

Fig. 10. *Rotor angle of Gitaru station for both wind farms.*

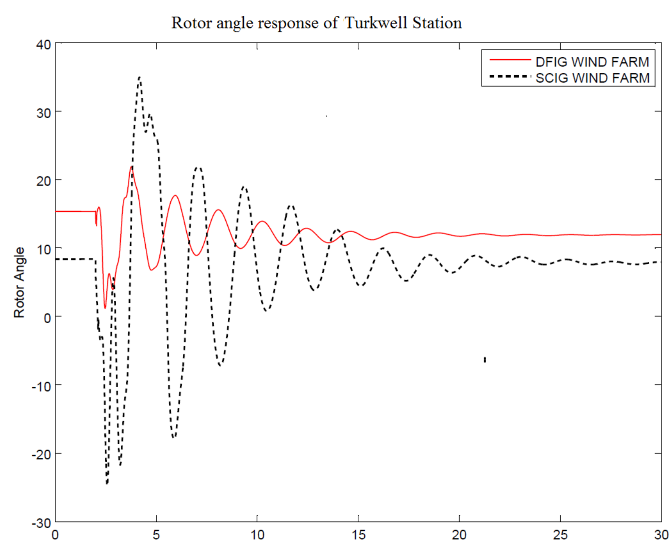

Fig. 11. *Rotor angle of Turkwell for both wind farms.*

It can be seen from Figures 10 and 11 that it the time it takes for the rotor angle response for the two power station is significantly reduced in the case of DFIG wind farm as compared to the SCIG based wind farm.

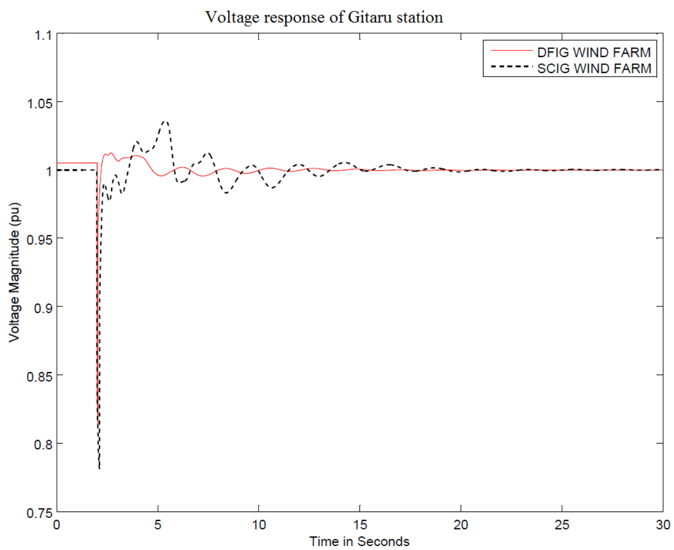

Fig. 12. *Voltage response of Gitaru for both wind farms.*

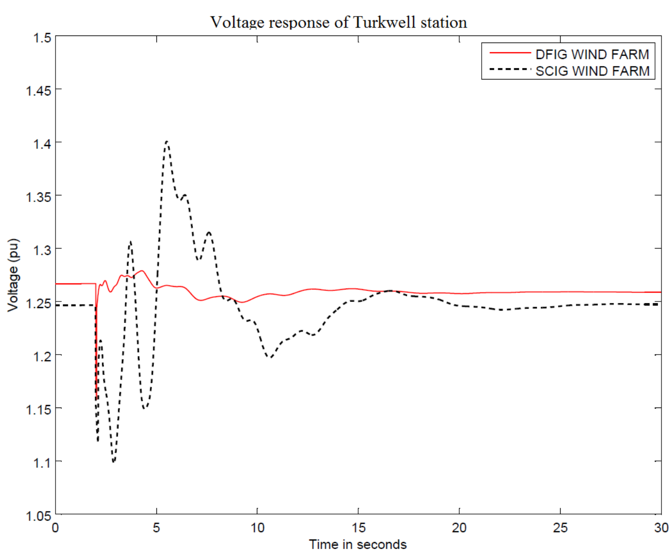

Fig. 13. *Voltage response of Turkwell for both wind farms.*

From Figures 12 and 13, it can be seen that with the inclusion of wind power from SCIG based wind farm, the voltage magnitude takes a longer time to settle after the fault. This is when compared to the case where the wind farm is replaced with an equivalent DFIG technology.
Similar results were also obtained when different generators were considered.

V. Conclusion

This paper investigated an efficient method of comparing impact of wind power from the two commonly used technologies on transient stability performance of a power system. The Kenyan power system modeled using the currently available data was used in this study. The performance of the system was observed when each of the two technologies were integrated each at a time. The performance of the system without wind power was studied first. Furthermore, the impact of power from wind considering two generator technologies was investigated one at a time. The results show that transient stability improves with DFIG based wind power integration. Our results agree with other published works for instance in Ch Eping et al [11].The findings in this paper provide useful information for the power system planning, especially the stakeholders in the Kenyan power system who are considering integrating this large wind farm into the system.

Acknowledgment

The authors would like to acknowledge the Pan African University, Institute Of Basic Sciences, Innovation and Technology for funding and facilitating the study.

References

[1] Wikipedia, the free encyclopedia, "Wind Power Capacity and Production," 2014.
[2] Global Wind Energy Council , "Global Wind Report of the year 2013," *GWEC Annual market update*, 2014.
[3] Jennifer DeCesaro and Kevin Porter, "Wind Energy and Power System Operations: A Review of Wind Integration Studies to Date," *National Renewable Energy Laboratory (NREL)*, December 2009.
[4] Xia Chen, Haishun Sun, Jinyu Wen, Wei-Jen Lee, Xufeng Yuan, Naihu Li, and Liangzhong Yao, "Integrating Wind Farm to the Grid Using Hybrid Multiterminal HVDC Technology," *IEEE Transactions on Industry Applications*, vol. 47, pp. 965 – 972, MARCH/APRIL March-April 2011.
[5] Lake Turkana Wind Project, "Power Generation - Kenya Power Sector," http://ltwp.co.ke/the-project/power-generation.
[6] *The Energy Act of Kenya*. Government of Kenya, 2006.
[7] M. Godoy Simes, Sudipta Chakraborty, and Robert Wood, "Induction Generators for Small Wind Energy Systems," IEEE Power Electronics Society NEWSLETTER, October 2006.
[8] Dr M S R Murty, "Wind Turbine Generator Model.".
[9] Anca D. Hansen, Florin Iov, Poul Srensen, Nicolaos Cutululis, Clemens Jauch, and Frede Blaabjerg, "Dynamic wind turbine models in power system simulation tool digsilent," tech. rep., Technical University of Denmark, August 2007.
[10] Markus A. Poller, "Doubly-fed induction machine models for stability assessment of wind farms," in *IEEE Power Tech Conference Proceedings*, Bologna, Italy, 26-30 July 2009.
[11] Ch. Eping, J. Stenzel, M. Poller, and H. Muller, "Impact of Large Scale Wind Power on Power System Stability," *Institute of Electrical Power Systems (IEPS)*, 2008.